Taylor & Francis
Taylor & Francis Group

Vehicle System Dynamics
International Journal of Vehicle Mechanics and Mobility

ISSN: 0042-3114 (Print) 1744-5159 (Online) Journal homepage: https://www.tandfonline.com/loi/nvsd20

# Suspension parameter estimation in the frequency domain using a matrix inversion approach

A. N. Thite , S. Banvidi , T. Ibicek & L. Bennett

**To cite this article:** A. N. Thite , S. Banvidi , T. Ibicek & L. Bennett (2011) Suspension parameter estimation in the frequency domain using a matrix inversion approach, Vehicle System Dynamics, 49:12, 1803-1822, DOI: 10.1080/00423114.2010.544319

**To link to this article:** https://doi.org/10.1080/00423114.2010.544319

*Vehicle System Dynamics*
Vol. 49, No. 12, December 2011, 1803–1822

Taylor & Francis
Taylor & Francis Group

# Suspension parameter estimation in the frequency domain using a matrix inversion approach

A.N. Thite,* S. Banvidi, T. Ibicek and L. Bennett

*Department of Mechanical Engineering, School of Technology, Oxford Brookes University, Wheatley, Oxford OX33 1HX, UK*

(*Received 13 April 2010; final version received 27 November 2010; first published 24 June 2011*)

The dynamic lumped parameter models used to optimise the ride and handling of a vehicle require base values of the suspension parameters. These parameters are generally experimentally identified. The accuracy of identified parameters can depend on the measurement noise and the validity of the model used. The existing publications on suspension parameter identification are generally based on the time domain and use a limited degree of freedom. Further, the data used are either from a simulated 'experiment' or from a laboratory test on an idealised quarter or a half-car model. In this paper, a method is developed in the frequency domain which effectively accounts for the measurement noise. Additional dynamic constraining equations are incorporated and the proposed formulation results in a matrix inversion approach. The nonlinearities in damping are estimated, however, using a time-domain approach. Full-scale 4-post rig test data of a vehicle are used. The variations in the results are discussed using the modal resonant behaviour. Further, a method is implemented to show how the results can be improved when the matrix inverted is ill-conditioned. The case study shows a good agreement between the estimates based on the proposed frequency-domain approach and measurable physical parameters.

**Keywords:** suspension parameters; parameter estimation; matrix inversion; 4-post rig; frequency domain; modal behaviour

## 1. Introduction

The components of the vehicle suspension system play a vital role in determining the vehicle handling and ride performance. The requirements of ride and handling are contradictory. The level of compromise depends on the application, e.g. a racing or primarily as a transport. The emphasis of vehicle suspension optimisation is put on the ride comfort on road cars and on the grip or minimisation of the contact patch variation on racing cars [1,2]. Because there are compliant, dissipative and inertial elements in any vehicle suspension system, resonance behaviour is seen based on the nature of excitation through tyres. The ride and handling are affected by this resonant behaviour. The optimisation process used to achieve balance between the handling and the ride can be entirely experimental-based or based only on theoretical simulations or a combination of them. In the automotive industry, the handling and

*Corresponding author. Email: athite@brookes.ac.uk

ISSN 0042-3114 print/ISSN 1744-5159 online

http://dx.doi.org/10.1080/00423114.2010.544319
http://www.tandfonline.com

ride compromise is often based on an experimental approach, demanding hours of expensive tests.

In theoretical and experimental studies, a vehicle is represented as a lumped parameter model, where the suspension system is idealised to comprise springs, viscous dampers and inertias. If only the vehicle bounce and pitch motions are of interest, the model can be built with four degrees of freedom (DOFs), which is a representation of the half-car model. If the roll is to be considered, the model will consist of seven DOFs, i.e. resulting in a full-car model. The idealisation of components as lumped parameters requires *a priori* knowledge of the parameters. The process becomes complex as, in particular, stiffness and mass are distributed across the vehicle structure and damping concentrated in some places. For example, one of the lumped parameters required is the unsprung mass which is formed from mass contribution from the wheel hub, tyre, spring, damper and any associated linkages. The contributions depend in a complex way on the mass and stiffness distribution. It becomes imperative to estimate these parameters indirectly. Apart from the requirement of these parameters for modelling at the design stage, these parameters are often required for vehicle re-engineering.

For an indirect estimation of the parameters, input and output response relationship can be used. This relationship is a complex function of mass, stiffness, damping and input frequency. One of the aims of parameter estimation techniques is to overcome these complexities to accurately estimate the system parameters. In the design stage, a solid model assembly could be created and using a multibody dynamics software, the responses could be estimated for particular inputs. The difficulty with this approach is the ability to model vehicle dynamic systems accurately, i.e. (a) how accurate is the model used (i.e. does it replicate an assembled vehicle? is the tyre modelled as required? are all the details included? etc.) and (b) how easy it is to simulate the responses accurately?

Suspension parameter estimation has been an active field of research; various techniques or methods of estimating vehicle suspension parameters [3–6] have been developed. Most of these techniques require vehicle suspension systems to be excited using a shaker rig or a poster rig that replicate road inputs. These approaches use sensors to measure accelerations and displacements at locations on some of the vehicle suspension components. In some studies, numerically simulated 'experiments' were used [3]. The validity of these techniques to estimate the suspension parameters is very much dependent on the number of DOFs employed, as well as on how well the influence of the measurement noise is reduced.

For instance, in [3], a time-domain approach was used to estimate eight vehicle parameters: overall sprung mass, front unsprung mass, rear unsprung mass, front spring stiffness, rear spring stiffness, front damping coefficient, rear damping coefficient and vehicle inertia. Further, a least-square (LS) approach was employed to reduce the errors in the estimations based on a four-DOF model. The results were based on the numerically simulated responses to random wheel inputs and not on the experiments on the vehicle; response-contaminating measurement noise was not accounted for. In the article, essentially, a matrix-inversion approach was used in obtaining the parameters. The form of matrix being inverted can have a significant influence on the errors in estimations. It is expected that the elements of the matrix would be related, and therefore, the matrix could be ill-conditioned. The system used was inherently under-determined as only four measured responses were used to obtain eight parameters, which makes the process more susceptible to any influence from the measurement noise.

In [4], a four-DOF model was used to estimate the same eight major vehicle suspension parameters in the time domain. The method used was based on the sliding observer and LS techniques. The measurements from a laboratory-based half-car test rig were used to show the validity of the method. In validating the approach, a damper curve was identified. This method, however, required the tyre stiffness to be known beforehand.

In [5,6], a two-DOF quarter-car model was used to estimate some of the vehicle parameters in the time domain. In [5], the approach was based on the use of two sensors measuring the sprung mass (body) acceleration and suspension displacement; it was claimed that sufficient details were available to estimate the nonlinear and linear characteristics of dampers with satisfactory accuracy. Here, again the method was not applied to measured data on a vehicle.

In [6], the damping coefficient and spring stiffness were estimated in the time domain. Here, the sprung and unsprung masses were assumed known. The damper and spring characteristics were determined, using the LS techniques. In using the approach, many of the responses were numerically integrated or differentiated as required. The sampling rate of data acquisition was suggested to play a crucial role in determining the accuracy of estimations. The paper also proposed a method for the estimation of road inputs.

All the papers reviewed here use the time-domain approaches. In this paper, a method is developed which can be implemented in either the time or the frequency domain. The proposed use of frequency content in combination with a frequency response estimator can reduce the effects of the measurement noise. The modal behaviour of the whole vehicle can then be used to assess the accuracy of the estimated parameters. The method proposed is a straightforward implementation of indirect, matrix-inversion-based parameter-estimation approach. Using a four-DOF system in either the time domain or the frequency domain, 10 vehicle suspension parameters, viz. sprung mass, front and rear unsprung masses, front and rear suspension spring stiffnesses, front and rear suspension damping coefficients, front and rear tyre stiffnesses and pitch inertia are estimated. The measurements of sprung and unsprung mass accelerations, angular response of the body, input forces and acceleration with respect to the road inputs generated on the 4-post rig are used for the purpose. The dynamic model developed is so arranged that all suspension parameters, measured signals and forces can be placed in three respective matrices. This allows estimation of the vehicle suspension parameters by the matrix-inversion approach and results in an LS solution.

In what follows, initially responses, parameters and forces are arranged in such a way as to obtain the response matrix, the parameter vector and the force vector at any instant of time. In one of the approaches, to account for noise in the measurements, the response matrix and the force vector are rearranged to be represented as accelerances (a ratio of acceleration to force), mobilities (a ratio of velocity to force) and receptances (a ratio of displacement to force) and force transmissibilities. To estimate these frequency responses, the $H_1$ [7] estimator is used. The time and the frequency-domain approaches are then implemented on the measured data on a car set-up on the 4-post rig. Further, a method, based on the Tikhonov matrix regularisation, is proposed by which the matrix ill-conditioning effects can be reduced [8–10]. Later, a method to estimate damping in the time domain is implemented using the knowledge of mass and stiffness parameters already obtained in the frequency domain. Finally, the parameters estimated using the time- and the frequency-domain methods are presented.

## 2. Formulation to estimate suspension system parameters

The approach developed in this paper is based on a four-DOF model (half-car model) of a vehicle by considering only the bounce and pitch motion. The schematic shown in Figure 1, in terms of unsprung mass, body or sprung mass, pitch inertia, suspension stiffness, suspension damping and tyre stiffness, is used for dynamic analysis. The equations obtained and found in common references are augmented by constraining equations in formulating the problem of parameter estimation.

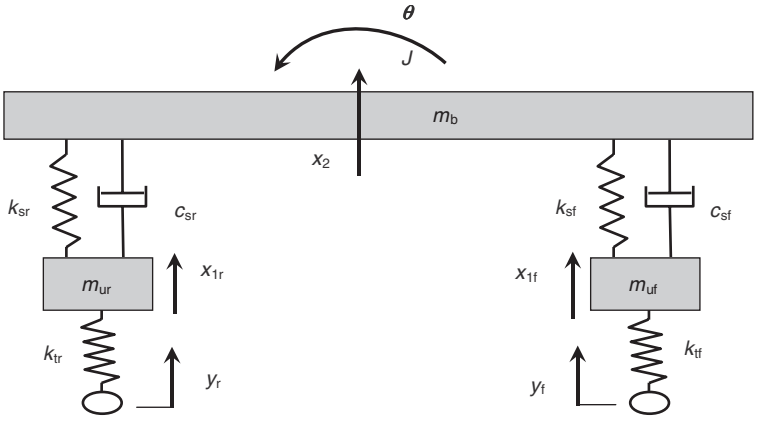


Figure 1. Lumped parameter half-car model.

The four-DOF model used has the following equations of motion written in the matrix form:

$$[\mathbf{M}]\{\ddot{\mathbf{x}}\} + [\mathbf{C}]\{\dot{\mathbf{x}}\} + [\mathbf{K}]\{\mathbf{x}\} = \{\mathbf{F}\}, \tag{1}$$

where

$$\mathbf{M} = \begin{bmatrix} m_b & 0 & 0 & 0 \\ 0 & J & 0 & 0 \\ 0 & 0 & m_{uf} & 0 \\ 0 & 0 & 0 & m_{ur} \end{bmatrix}, \quad \mathbf{K} = \begin{bmatrix} k_{sf}+k_{sr} & k_{sf}l_1 - k_{sr}l_2 & -k_{sf} & -k_{sr} \\ k_{sf}l_1 - k_{sr}l_2 & k_{sf}l_1^2 + k_{sr}l_2^2 & -k_{sf}l_1 & k_{sr}l_2 \\ -k_{sf} & -k_{sf}l_1 & k_{sf}+k_{tf} & 0 \\ -k_{sr} & k_{sr}l_2 & 0 & k_{sr}+k_{tr} \end{bmatrix},$$

$$\mathbf{C} = \begin{bmatrix} c_{sf}+c_{sr} & c_{sf}l_1 - c_{sr}l_2 & -c_{sf} & -c_{sr} \\ c_{sf}l_1 - c_{sr}l_2 & c_{sf}l_1^2 + c_{sr}l_2^2 & -c_{sf}l_1 & c_{sr}l_2 \\ -c_{sf} & -c_{sf}l_1 & c_{sf}+c_{tf} & 0 \\ -c_{sr} & c_{sr}l_2 & 0 & c_{sr}+c_{tr} \end{bmatrix},$$

$$\mathbf{x} = \begin{Bmatrix} x_2 \\ \theta \\ x_{1f} \\ x_{1r} \end{Bmatrix} \quad \text{and} \quad \mathbf{F} = \begin{Bmatrix} 0 \\ 0 \\ k_{tf}y_f \\ k_{tr}y_r \end{Bmatrix},$$

where $m_b$ is the sprung or body mass, $J$ the pitch inertia, $k_{sf}$ the front suspension stiffness, $k_{sr}$ the rear suspension stiffness, $c_{sf}$ the front suspension damping coefficient, $c_{sr}$ the rear suspension damping coefficient, $m_{uf}$ the front unsprung mass, $m_{ur}$ the rear unsprung mass, $k_{tf}$ the front tyre stiffness and $k_{tr}$ the rear tyre stiffness. The response variables used are: $\theta$, the pitch angular displacement; $x_2$, the body bounce motion; $x_{1f}$, the displacement of front unsprung mass; and $x_{1r}$, the displacement of rear unsprung mass. The displacement inputs at front and rear tyre contacts with ground are represented by $y_f$ and $y_r$, respectively. The equations of motion above are valid for small pitch angular displacement; nonlinear terms are required for accurate representation if large displacements occur. In this application, the assumption of small angular displacement does not result in large errors.

There are three more constraining equations that can be obtained which relate to the inertial parameters using dynamic and static equilibrium conditions. For the dynamic condition, constraining equations are given by

$$\begin{aligned} m_{\mathrm{b}}\ddot{x}_2 + m_{\mathrm{uf}}\ddot{x}_{1\mathrm{f}} + m_{\mathrm{ur}}\ddot{x}_{1\mathrm{r}} &= k_{\mathrm{tf}}(y_{\mathrm{f}} - x_{1\mathrm{f}}) + k_{\mathrm{tr}}(y_{\mathrm{r}} - x_{1\mathrm{r}}) \\ J\ddot{\theta} + m_{\mathrm{uf}}\ddot{x}_{1\mathrm{f}}l_1 - m_{\mathrm{ur}}\ddot{x}_{1\mathrm{r}}l_2 &= k_{\mathrm{tf}}(y_{\mathrm{f}} - x_{1\mathrm{f}})l_1 - k_{\mathrm{tr}}(y_{\mathrm{r}} - x_{1\mathrm{r}})l_2. \end{aligned} \tag{2}$$

Under the static equilibrium condition, the equation obtained is given below:

$$\begin{aligned} & m_{\mathrm{b}}g + m_{\mathrm{uf}}g + m_{\mathrm{ur}}g = Mg \\ \Longrightarrow\ & m_{\mathrm{uf}} = M - (m_{\mathrm{ur}} + m_{\mathrm{b}}). \end{aligned} \tag{3}$$

In the above equations, for known input forces and output responses (accelerations, velocities and displacements), the expressions can be rearranged to obtain parameters of the system. The rearrangement achieved is similar to that given in [3], but with additional constraining equations (2) and (3). Initially, the method developed is implemented in the time domain and corresponding formulation is developed in the next section. Later, a new frequency-domain approach is developed.

### 2.1. *Implementation in the time domain*

Observing Equations (1)–(3), there are 10 parameters of the vehicle system that are in use. As the weight of the car is known (hence the mass $M$) from static load cell measurements, there are two unknown masses in Equation (3) (i.e. $m_{\mathrm{ur}}$ and $m_{\mathrm{b}}$) rather than three. Therefore, there are nine ($k_{\mathrm{tf}}$, $k_{\mathrm{tr}}$, $k_{\mathrm{sf}}$, $k_{\mathrm{sr}}$, $c_{\mathrm{sf}}$, $c_{\mathrm{sr}}$, $m_{\mathrm{b}}$, $m_{\mathrm{ur}}$ and $J$) independent system parameters that need to be identified. Out of these, four stiffnesses can be estimated by knowing the ratios of input force to output displacement or reciprocal of them. At low frequencies (where inertial and damping influence within the tyres is minimal), the tyre stiffnesses can be estimated as

$$k_{\mathrm{tf}} \approx \frac{F_{\mathrm{f}}}{y_{\mathrm{f}} - x_{1\mathrm{f}}}; \quad k_{\mathrm{tr}} \approx \frac{F_{\mathrm{r}}}{y_{\mathrm{r}} - x_{1\mathrm{r}}}, \tag{4}$$

where $F_{\mathrm{f}}$ and $F_{\mathrm{r}}$ are the measured forces at the contact between ground and tyre for front and rear wheels, respectively. Similarly, using part of Equation (1), at low frequencies, the suspension stiffnesses can be estimated as

$$k_{\mathrm{sf}} \approx \frac{F_{\mathrm{f}}}{x_{1\mathrm{f}} - (x_2 + l_1\theta)}; \quad k_{\mathrm{sr}} \approx \frac{F_{\mathrm{r}}}{x_{1\mathrm{r}} - (x_2 - l_2\theta)}. \tag{5}$$

Based on the information available, now there are only five independent parameters left to be estimated in Equation (1). As a first step in estimating the remaining suspension parameters, using Equations (1)–(3), the expression can be rearranged so that the unknown and known parameters are separated; further manipulations lead to the following form:

$$[\mathbf{A}(\ddot{x}, \dot{x}, x)]\{\mathbf{P}(m, c, k)\} = \{\mathbf{F}\}, \tag{6}$$

where

$$[\mathbf{A}(\ddot{x},\dot{x},x,\ddot{\theta},\dot{\theta},\theta)]=\begin{bmatrix} \ddot{x}_2 & 0 & 0 & \dot{x}_2-\dot{x}_{1\mathrm{f}}+l_1\dot{\theta} & \dot{x}_2-\dot{x}_{1\mathrm{r}}-l_2\dot{\theta} \\ 0 & \ddot{\theta} & 0 & (\dot{x}_2-\dot{x}_{1\mathrm{f}}+l_1\dot{\theta})l_1 & (-\dot{x}_2+\dot{x}_{1\mathrm{r}}+l_2\dot{\theta})l_2 \\ -\ddot{x}_{1\mathrm{f}} & 0 & -\ddot{x}_{1\mathrm{f}} & \dot{x}_{1\mathrm{f}}-\dot{x}_2-l_1\dot{\theta} & 0 \\ 0 & 0 & \ddot{x}_{1\mathrm{r}} & 0 & \dot{x}_{1\mathrm{r}}-\dot{x}_2+l_2\dot{\theta} \\ \ddot{x}_2-\ddot{x}_{1\mathrm{f}} & 0 & \ddot{x}_{1r}-\ddot{x}_{1\mathrm{f}} & 0 & 0 \\ -\ddot{x}_{1\mathrm{f}}l_1 & \ddot{\theta} & -\ddot{x}_{1\mathrm{r}}l_2+\ddot{x}_{1\mathrm{f}}l_1 & 0 & 0 \end{bmatrix},$$

$$\mathbf{P}(m,c,k)=\begin{Bmatrix} m_{\mathrm{b}} & J & m_{\mathrm{ur}} & c_{\mathrm{sf}} & c_{\mathrm{sr}} \end{Bmatrix}^{\mathrm{T}},$$

$$\mathbf{F}=\begin{Bmatrix} k_{\mathrm{sf}}(-x_2+x_{1\mathrm{f}}-l_1\theta)+k_{\mathrm{sr}}(-x_2+x_{1\mathrm{r}}+l_2\theta) \\ k_{\mathrm{sf}}(-x_2+x_{1\mathrm{f}}-l_1\theta)l_1+k_{\mathrm{sr}}(x_2-x_{1\mathrm{r}}-l_2\theta)l_2 \\ k_{\mathrm{sf}}(x_2-x_{1\mathrm{f}}+l_1\theta)+F_{\mathrm{f}}-M\ddot{x}_{1\mathrm{f}} \\ k_{\mathrm{sr}}(x_2-x_{1\mathrm{r}}-l_2\theta)+F_{\mathrm{r}} \\ F_{\mathrm{f}}+F_{\mathrm{r}}-M\ddot{x}_{1\mathrm{f}} \\ F_{\mathrm{f}}l_1-F_{\mathrm{r}}l_2-M\ddot{x}_{1\mathrm{f}}l_1 \end{Bmatrix}.$$

Equation (6) is formed by collecting (a) all known forces resulting from various known parameters and inputs to the right-hand side giving rise to the forcing vector **F**, (b) known responses to form the response matrix **A** and (c) unknowns to form the parameters vector **P**. The unknown parameters can be estimated readily by pre-multiplying both sides of Equation (6) by the inverse of the response matrix **A**. The response matrix above is rectangular and hence cannot be inverted straightforwardly; however, in the LS sense pseudo inverse [8] can be obtained. Therefore, by rearranging Equation (6), the expression for system parameters can be written as follows:

$$\{\mathbf{P}(m,c,k)\}=[\mathbf{A}(\ddot{x},\dot{x},x)]^{+}\{\mathbf{F}\}, \tag{7}$$

where $[\mathbf{A}(\ddot{x},\dot{x},x)]^{+}$ is the Moore–Penrose pseudo inverse of the rectangular matrix **A**. The expression of which is given by

$$[\mathbf{A}(\ddot{x},\dot{x},x)]^{+}=([\mathbf{A}(\ddot{x},\dot{x},x)]^{\mathrm{T}}[\mathbf{A}(\ddot{x},\dot{x},x)])^{-1}[\mathbf{A}(\ddot{x},\dot{x},x)]^{\mathrm{T}}, \tag{8}$$

where $\bullet^{\mathrm{T}}$ is the transpose of the concerned matrix. Note that the right-hand side of Equation (8) is time-dependent and consequently so does the left-hand side. When measurements are performed to obtain vehicle system responses, matrices **A** and **F** can be constructed at every instant of sampled time. The measured responses are always affected by the measurement noise. There is also the effect of the high-frequency contamination due to the dynamics of combination of the test rig and the vehicle. Appropriate filtering techniques can be used to reduce the effect of the high-frequency contamination. The filtering techniques in most cases, however, cannot remove this type of noise completely and in fact, in some cases, the bias introduced during the filtering may make the situation worse. Random noise present in measured responses can also be a concern as Equation (7) involves the matrix inversion, which can magnify the noise effects in measured responses. In the next section, an alternative approach for reducing the effect of noise in the measured responses is presented; it is a frequency-domain approach. Later in Section 5, results from the time domain and the frequency domain are compared.

### 2.2. *Implementation in the frequency domain*

One way of reducing the measurement noise is by writing the equations in the matrix form as frequency response functions, with one of the measurements taken as a reference; this

can reduce the effect of random noise in estimated response functions. Consequent to this representation, the estimated parameters will be functions of frequencies. The influence of higher frequency content will be of no concern in this approach. The available frequency response function estimators can reduce the effect of either input or output noise. The $H_1$ estimator used here reduces the effect of noise on the output. There is, however, a disadvantage in using the frequency-domain approach; the nonlinearities cannot be identified that easily. This will have an influence on the estimated value of the nonlinear parameters such as damping values. In any case, at the first instance, the estimates of all the parameters can be obtained in the frequency domain and then the damping values can be updated based on the hysteresis curve. Details of damping estimations are given later in this paper.

The stiffnesses obtained in the time domain as ratios of transmitted forces to relative displacements can also be obtained by similar implementation in the frequency domain, but as frequency response functions. For example, the front suspension stiffness can be estimated as a frequency response function between suspension force and suspension displacement by taking the suspension displacement as a reference:

$$k_{\mathrm{sf}}(\omega) \approx \frac{F_{\mathrm{f}}(\omega)}{z_{\mathrm{f}}(\omega)} = H_{F_{\mathrm{f}}z_{\mathrm{f}}}(\omega), \tag{9}$$

where $H_{F_{\mathrm{f}}z_{\mathrm{f}}}(\omega)$ is a frequency response function and $\omega$ the radian frequency. The subscripts used in the frequency response function are in the sequence of the output variable and followed by the reference input. Later on in the paper, the subscript representing reference will be removed with the understanding that the same reference is used in a particular formula on all variables. In Equation (9), the effects of nonlinearity are neglected; it is assumed here that the displacements are small and hence the nonlinearities in stiffnesses are negligible.

With the knowledge of the values of stiffnesses, the frequency-domain representation to estimate other parameters can be derived; it is given below (the reference used is the front wheel force at contact between ground and wheel).

$$[\mathbf{A}_\omega(\ddot{x}, \dot{x}, x)]\{\mathbf{P}_\omega(m, c, k)\} = \{\mathbf{F}_\omega\}, \tag{10}$$

where

$$[\mathbf{A}_\omega(\ddot{x}, \dot{x}, x, \ddot{\theta}, \dot{\theta}, \theta)]$$

$$= \omega^2 \begin{bmatrix} H_{X_2} & 0 & 0 & j\dfrac{(H_{X_2} - H_{X_{1\mathrm{f}}} + l_1 H_\theta)}{\omega} & j\dfrac{(H_{X_2} - H_{X_{1\mathrm{r}}} + l_2 H_\theta)}{\omega} \\ 0 & H_\theta & 0 & j\dfrac{(H_{X_2} - H_{X_{1\mathrm{f}}} + l_1 H_\theta)}{\omega} l_1 & j\dfrac{(H_{X_{1\mathrm{r}}} - H_{X_2} + l_2 H_\theta)}{\omega} l_2 \\ -H_{X_{1\mathrm{f}}} & 0 & -H_{X_{1\mathrm{f}}} & j\dfrac{(H_{X_{1\mathrm{f}}} - H_{X_2} - l_1 H_\theta)}{\omega} & 0 \\ 0 & 0 & H_{X_{1\mathrm{r}}} & 0 & j\dfrac{(H_{X_{1\mathrm{r}}} - H_{X_2} + l_2 H_\theta)}{\omega} \\ (H_{X_2} - H_{X_{1\mathrm{f}}}) & 0 & (H_{X_{1\mathrm{r}}} - H_{X_{1\mathrm{f}}}) & 0 & 0 \\ -H_{X_{1\mathrm{f}}} l_1 & H_\theta & (H_{X_{1\mathrm{f}}} l_1 - H_{X_{1\mathrm{r}}} l_2) & 0 & 0 \end{bmatrix},$$

$$\mathbf{P}_\omega(m,c,k) = \left\{ m_{\mathrm{b}}(\omega) \quad J(\omega) \quad m_{\mathrm{ur}}(\omega) \quad c_{\mathrm{sf}}(\omega) \quad c_{\mathrm{sr}}(\omega) \right\}^{\mathrm{T}},$$

$$\mathbf{F}_\omega = \begin{Bmatrix} k_{\mathrm{sf}}(-H_{X_2} + H_{X_{1\mathrm{f}}} - l_1 H_\theta) + k_{\mathrm{sr}}(-H_{X_2} + H_{X_{1\mathrm{r}}} + l_2 H) \\ k_{\mathrm{sf}}(H_{X_{1\mathrm{f}}} - H_{X_2} - l_1 H_\theta) l_1 + k_{\mathrm{sr}}(H_{X_2} - H_{X_{1\mathrm{r}}} - l_2 H_\theta) l_2 \\ k_{\mathrm{sf}}(H_{X_2} - H_{X_{1\mathrm{f}}} + l_1 H_\theta) + 1 + \omega^2 M H_{X_{1\mathrm{f}}} \\ k_{\mathrm{sr}}(H_{X_2} - H_{X_{1\mathrm{r}}} - l_2 H_\theta) + H_{\mathrm{F_r}} \\ 1 + H_{\mathrm{F_r}} + \omega^2 M H_{X_{1\mathrm{f}}} \\ l_1 + H_{\mathrm{F_r}} l_2 + \omega^2 M H_{X_{1\mathrm{f}}} l_1 \end{Bmatrix}. \tag{11}$$

The matrix $\mathbf{A}_\omega$ contains frequency response functions of accelerances, mobilities and receptances which contain both the phase and the amplitude information. Using the approach as used earlier in the time-domain implementation, the solution for parameters can be written as

$$\{\mathbf{P}_\omega(m,c,k)\} = [\mathbf{A}_\omega(\ddot{x},\dot{x},x)]^{+}\{\mathbf{F}_\omega\}. \tag{12}$$

The parameters estimated above may show frequency dependence and there could also be some errors present due to the matrix inversion. The errors in estimated parameters will depend on the condition number of the matrix $\mathbf{A}_\omega$ and the remaining measurement noise in frequency response functions. If condition numbers are large, the errors in estimations could mask the actual values of parameters. The difficulty can be overcome by the use of some forms of the matrix regularisation [8,9] while inverting the matrix $\mathbf{A}_\omega$. In Section 2.3, one such method is briefly discussed.

### 2.3. *The effect of matrix condition number on the estimated parameters*

The frequency response function matrix in the frequency-domain approach, as well as the response matrix in the time-domain approach, can show a variation in condition numbers. When a mode (e.g. pitch mode) of a vehicle is excited, the responses measured at all points can be dominated by this mode, which in the matrix algebra means partially or fully correlated elements in the matrix. Consequently, the matrix would not be full rank, which also means increased condition numbers. Increased condition numbers can result in larger errors in estimated parameters. However, the errors in all the parameters may not be the same.

One way of overcoming this problem is by regularising the matrix being inverted; well-known Tikhonov [8,9] regularisation can be used. Similar applications of matrix regularisation can be found in force identification problems of structural dynamics [10]. After applying such regularisation, the solution to parameters can be written as

$$\{\mathbf{P}_\omega(m,c,k)\} = ([\mathbf{A}_\omega(\ddot{x},\dot{x},x)]^{\mathrm{T}}[\mathbf{A}_\omega(\ddot{x},\dot{x},x)] + I\lambda)^{-1}[\mathbf{A}_\omega(\ddot{x},\dot{x},x)]^{\mathrm{T}}\{\mathbf{F}_\omega\}. \tag{13}$$

The important factor that decides how well the parameters are estimated is the choice of the regularisation parameter, $\lambda$. There are several ways [9] in which the regularisation parameter can be chosen; however, the selection method to choose the regularisation parameter is not the object of this paper. For the purpose of this paper, just one value of the regularisation parameter is used to demonstrate the effectiveness.

## 3. Experiments using a 4-post rig

A 4-post rig was used to measure responses on the vehicle. Specific inputs were generated on the 4-post rig's wheel pans, on which tyres rest. Each wheel pan is connected to a vertical hydraulic actuator controlled by a central control system, allowing the achievement of the required

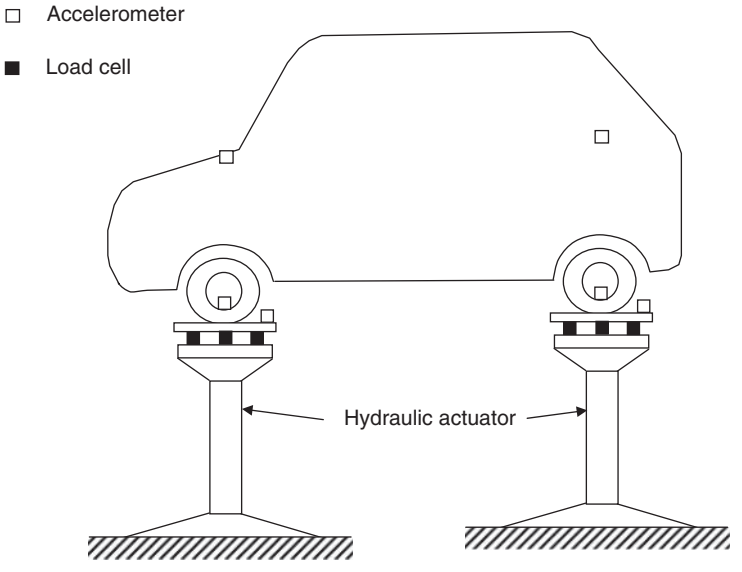


Figure 2. Experimental arrangement showing the location of accelerometers and load cells in the 4-post rig testing.

vertical displacement of the actuators. The schematic of the transducer arrangement on the 4-post rig set-up is shown in Figure 2. The wheel pans sit on the four load cells which measure the forces applied to tyres and an accelerometer for each was also mounted on the wheel pans to measure the 'road input' accelerations. Further, four MEMS (MicroElectroMechanical Systems) accelerometers of the capacitive type were used for measuring the vibration responses of wheels and the vibration responses of the vehicle body. The signals of accelerometers connected to the vehicle body were manipulated to obtain the pitch motion about the centre of gravity and the body bounce motion of the centre of gravity.

The swept-sine wave was used as a road input to enable the estimation of the frequency responses of a vehicle. The amplitudes used were based on the fact that the road inputs [2] are expected to be of large displacement amplitudes for a large wavelength (low frequency) road variations and the amplitudes decrease for decreasing wavelength (larger frequency).

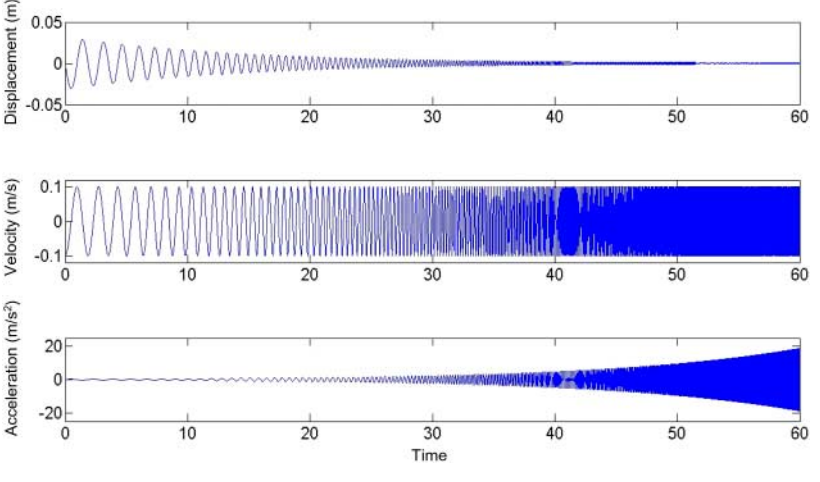


Figure 3. Sine sweep input used to generate wheel excitation on the 4-post rig.

To account for these variations, the velocity amplitude can be kept constant. Typical road input to wheels on the 4-post rig considering the above road characteristics, is shown in Figure 3. In 60 s time duration, the excitation frequency was swept from 0.5 to 30 Hz. The frequency range of interest for the vehicle used was limited by the vehicle's dynamical behaviour; the resonant behaviour of interest was covered by frequencies between 0.5 and 30 Hz. Based on this and considering the aliasing effect, the sampling rate of 200 Hz was used in the experiments. The time-history data from the 4-post rig was then post-processed using appropriate MATLAB functions.

## 4. Results from the tests using 4-post rig

### 4.1. *Time-domain results*

In the first place, the time-domain approach proposed in Section 2.1 was used to obtain system parameters. The matrix inversion was performed at every instant of time. Two of the raw data used to form the matrix **A** are shown in Figure 4. The signals are significantly contaminated by measurement noise and may also have been influenced by high-frequency behaviour (which is of no interest in this application). The Butterworth low pass filter was used to reduce noise in the measured signals, as well as to remove the higher frequency content. The filtered acceleration signal measured on the wheel pan is shown in Figure 4a; the signal looks much cleaner and random variations are reduced. The input signal used being sinusoidal, the difficulty in filtering the signal of Figure 4a was minimal. This may not always be the case; for example, the responses measured on the vehicle body can be a complex combination of resonant behaviour of the whole system.

The vehicle body mass and pitch inertia estimated using the time-domain approach are shown in Figure 5a and b. Both estimates show significant errors and the estimations vary in value throughout the time duration. Estimations of damping coefficients are shown in Figure 6a and b; the estimations show large errors. In the plot, there appears to be a line in the background around which the variations seem to occur. However, it is very difficult to reveal this line, which can be treated as estimated damping. One reason for large errors in estimated parameters in the time domain is that the response data contains noise and the matrix inverted may be ill-conditioned.

### 4.2. *Frequency-domain results*

In this approach, initially frequency response functions were estimated to generate elements of matrix $\mathbf{A}_\omega$. The frequency resolution of 0.25 Hz was chosen in order to avoid introduction of artificial damping. During post-processing, overlapping and the Hanning window were used as appropriate to reduce random noise and signal-processing effects. Figure 7 shows the frequency response function (in this case transmissibility) plots for the vehicle body bounce motion and the front unsprung mass motion. As the model considered has four DOFs, four resonant modes of vibration can contribute to the frequency response functions. These modes are: (a) body bounce mode, (b) body pitch mode, (c) front hub mode (which corresponds to the dominant motion of the front unsprung mass) and (d) rear hub mode (which corresponds to the dominant motion of the rear unsprung mass). Two peaks in the body bounce motion frequency response show an influence of the body bounce mode and the hub mode. The body bounce mode occurs around 1.75 Hz (which is much broader indicating the presence of larger damping and may have an influence from the pitch mode's proximity) and the hub mode occurs between 13

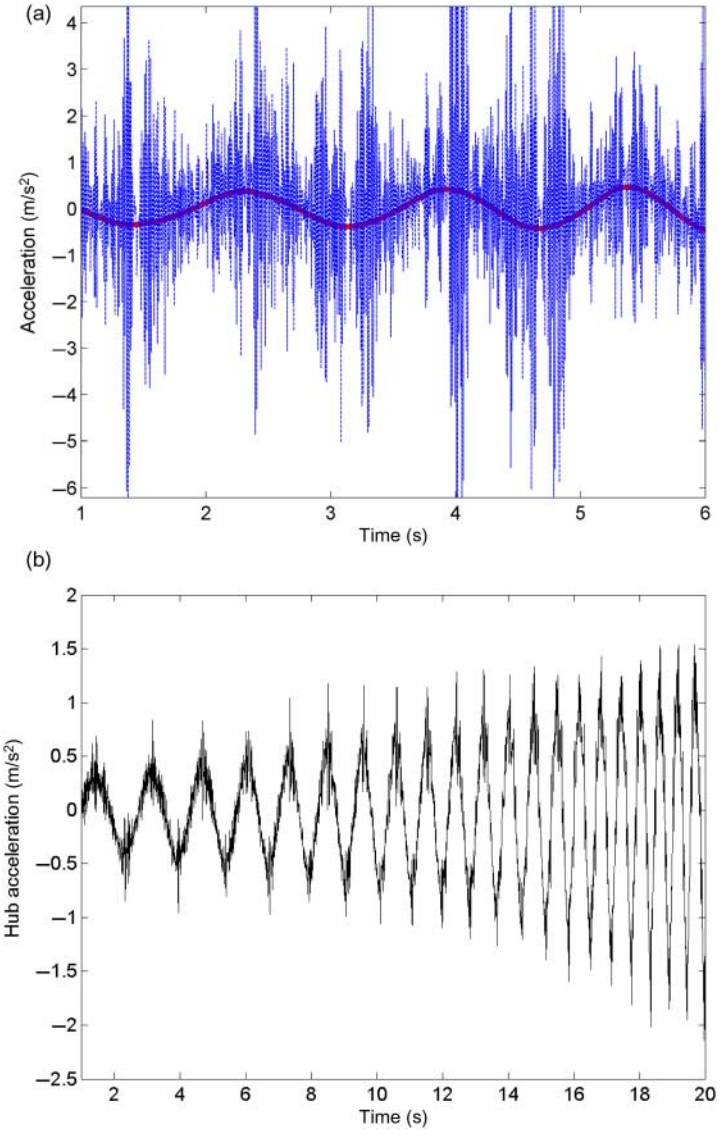


Figure 4. Noise in accelerations measured. (a) Acceleration measured at tyre contact (filtered signal is also shown as thick line). (b) Front unsprung mass acceleration.

and 14 Hz. Because of the presence of resonant peaks in the responses, the elements of matrix $\mathbf{A}_\omega$ are dependent on the resonant behaviour of the system. This behaviour may influence the accuracy of estimated parameters. Before analysing any results, the elements of matrix $\mathbf{A}_\omega$ are further investigated to understand the effect of dynamics on the matrix-inversion-based estimations.

To understand the contributions from different modes to the responses, the model resulting in Equation (1) was used with typical linear parameter values (the parameters used are listed in Table 1) to numerically simulate frequency response functions. The results of these numerical simulations are discussed next. The mode superposition principle was used to obtain the frequency responses. To highlight the resonant modes, the damping used in the numerical simulation was intentionally chosen smaller than that found in typical vehicles. In Figure 8,

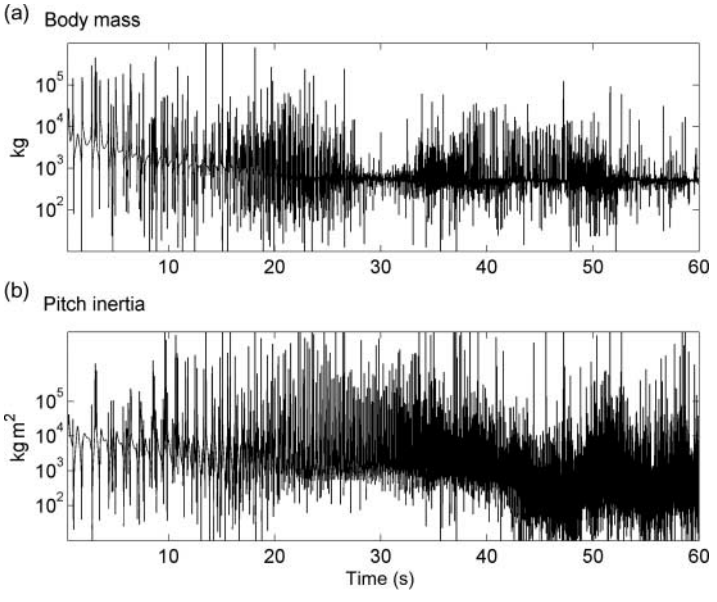


Figure 5. Estimated (a) body or sprung mass and (b) pitch inertia estimate using the time-domain approach.

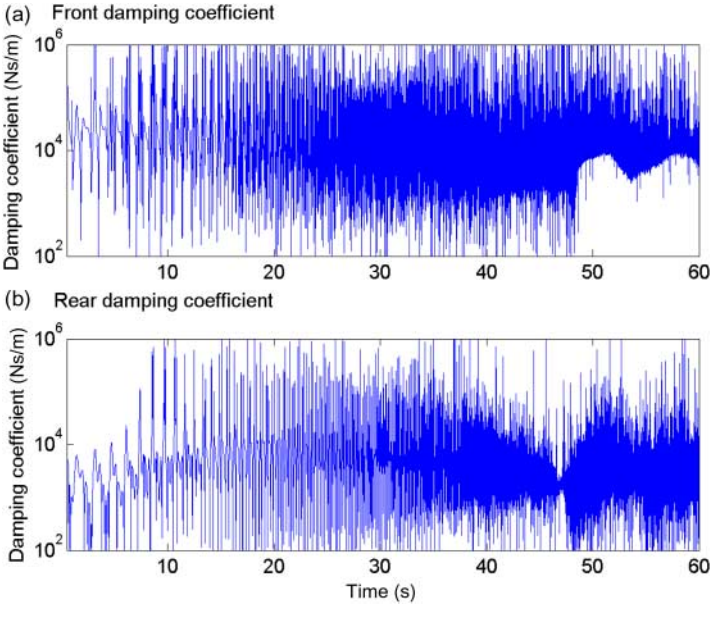


Figure 6. Estimated damping coefficient using the time-domain approach.

the body bounce response is shown. It is interesting to see the presence of two peaks around 2 Hz; the first peak is from the contribution of the body bounce mode and the second one is from the contribution of the pitch mode. The hub mode occurs further up the frequency and the peak associated is much smaller than the body bounce mode and the pitch mode. Modal contributions of each of the modes are also shown to clarify the significant contributions.

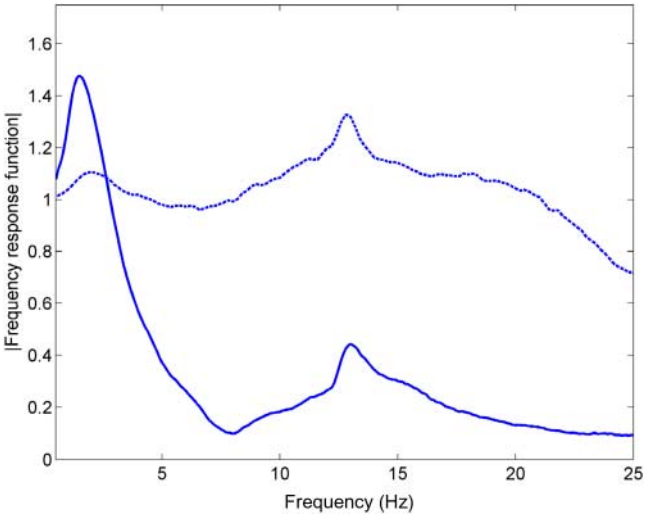


Figure 7. Measured frequency response functions (transmissibilities) with tyre displacement input taken as a reference. —, frequency response function of body motion; – –, frequency response function of unsprung mass motion.

Table 1. Parameters used in the simulation to find modal contribution; used in estimating responses of Figures 8–10.

| Parameter | Value |
|---|---|
| Body or sprung mass | 1020 kg |
| Pitch inertia | 1200 kg m$^2$ |
| Front unsprung mass | 36 kg |
| Rear unsprung mass | 36 kg |
| Front suspension stiffness | 48,000 N/m |
| Rear suspension stiffness | 48,000 N/m |
| Tyre stiffness | $4.4 \times 10^5$ N/m |
| Front damping coefficient | 500 Ns/m |
| Rear damping coefficient | 500 Ns/m |
| Length from centre of gravity to the front wheel | 0.9 m |
| Length from centre of gravity to the rear wheel | 1.53 m |

Similar plots can also be drawn for the unsprung mass responses. For example, in Figure 9, the front unsprung mass response is shown. As the damping values used were smaller than, practically present, the peaks here are exaggerated. Nevertheless, comparing Figures 8 and 9, the hub mode's dominance in the response of unsprung mass can be seen clearly. In Figure 10, the pitch response of the vehicle body is shown; the response is significantly smaller after $\sim$5 Hz in comparison to the body bounce motion (Figure 8) and the unsprung mass motion (Figure 9).

The resonant behaviour seen above means that the elements of matrix $\mathbf{A}_\omega$ (Equation (11)) at any frequency may be dominated by one or a few modes of vibrations, i.e. the matrix could be ill-conditioned. The matrix inversion, therefore, may not give out reliable estimates of all the parameters at all the frequencies. In general, however, the particular mode's dominance at a specific frequency can easily be found out; the estimates of parameters related to that mode would be reliable around the frequency range of dominance. For example, the hub mode has hardly any contribution to the responses below $\sim$12 Hz (Figures 8 and 10), where as the body bounce mode and the pitch mode contribute significantly at lower frequencies to

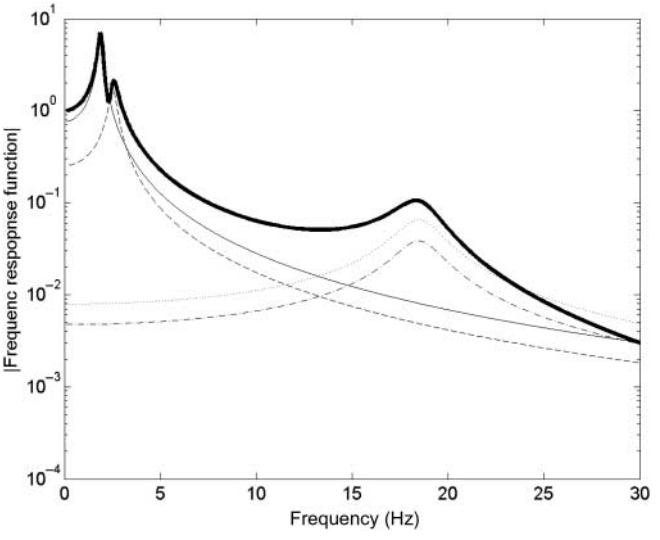


Figure 8. Modal contribution to bounce or heave motion of the vehicle body mass. ——, total response; —, bounce mode contribution; – –, pitch mode contribution; and – · – and ....., two hub mode contributions.

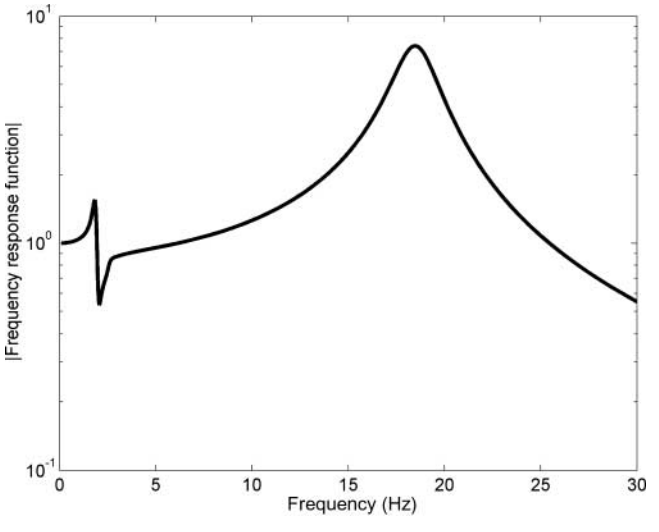


Figure 9. Front unsprung mass motion-based frequency response function (transmissibility). The effect of reduced damping can be clearly seen in increased peak at ∼15 Hz.

the body bounce and pitch motion. In addition, if the body bounce and pitch angle frequency response functions are compared: (a) the pitch mode contribution to the body bounce response is significant only between ∼2 and 5 Hz (Figure 8) and (b) the body bounce response appears significantly larger at higher frequencies (Figures 8 and 10). This discussion suggests, for example, that the estimates of the unsprung mass may not be reliable below ∼12 Hz and above ∼15 Hz. Similarly, the pitch inertia estimations may not be reliable for frequencies larger than ∼5 Hz.

With the understanding of the modal behaviour of the system, the results of parameter estimations can be discussed next. Figure 11 shows the body mass and the pitch inertia estimations. The pitch inertia estimations show significant variations. The matrix condition numbers and

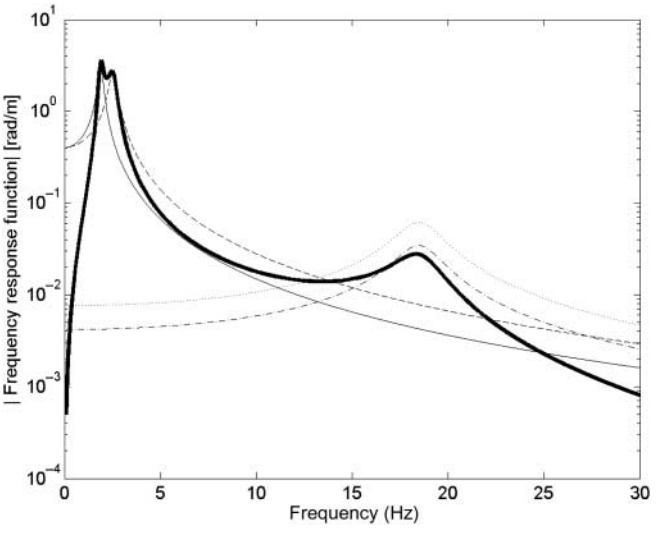


Figure 10. Modal contribution to the pitch motion of the vehicle body. ——, total pitch response; —, bounce mode contribution; – –, pitch mode contribution; – · – and ....., two hub mode contributions.

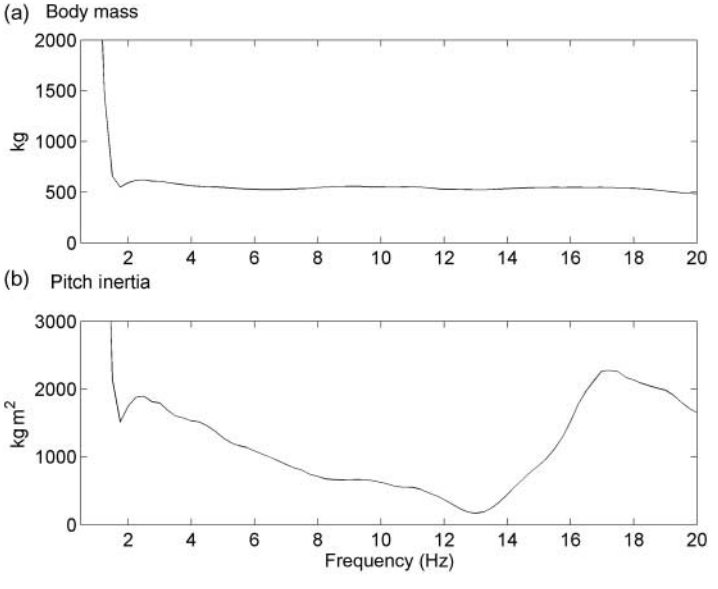


Figure 11. Estimated (a) body or sprung mass and (b) pitch inertia using the frequency-domain technique.

varying contribution from the pitch mode may have influenced this behaviour. The body mass estimated is constant after 5 Hz; below 2 Hz, there may be some influence of the matrix condition and the measurement noise. Figure 12 shows the effect of regularisation on the estimated body mass and pitch inertia. Here, the matrix was regularised using a nominal, small value (in this example, 0.0001) regularisation parameter. The value of the regularised parameter is much smaller than, for example, the highest singular value 0.00482 at the body bounce mode (1.75 Hz). The solution appears to improve the result between 2 and 5 Hz for the pitch inertia, making worse the results of the body mass for the frequencies below 5 Hz; the smaller of the parameters estimated getting adversely affected. This behaviour has been observed before in

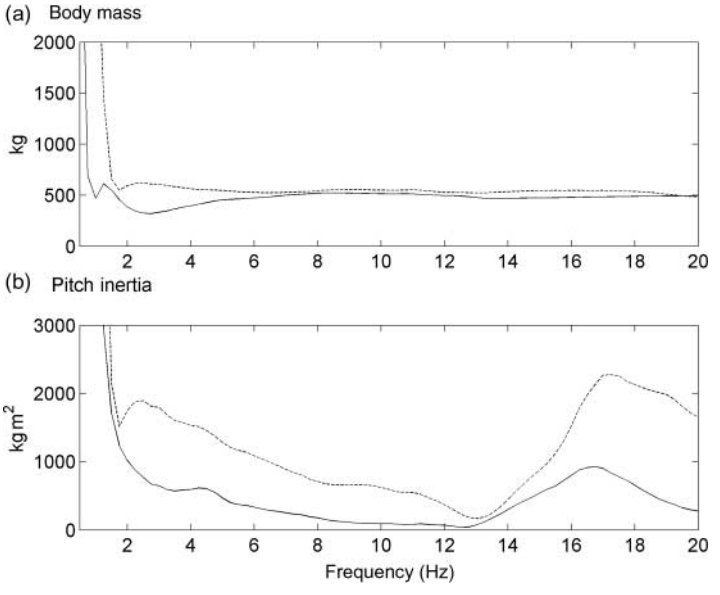


Figure 12. Estimated (a) body or sprung mass and (b) pitch inertia using the frequency-domain technique. —, regularised solution; – –, ordinary solution.

the field of force identification problems [10]. However, it is to be noted that with the appropriate choice of the regularisation parameter, a compromised estimate of the pitch inertia and the body mass could be obtained; the topic of selection of the appropriate value of regularisation will not be explored any further in this paper.

Figure 13 shows the estimated unsprung mass; as discussed before, the results between 13 and 15 Hz, where the hub mode is dominant, are comparable to typical values. A very small

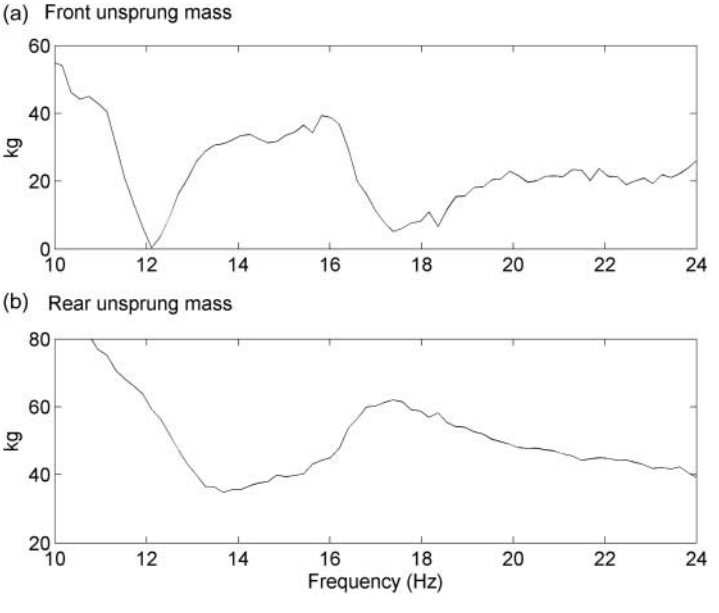


Figure 13. Estimated unsprung mass using the frequency-domain technique.

variation is seen in this frequency region. For all practical purposes, the frequency average of the values can be taken.

### 4.3. *Estimation of damping*

The damping coefficient estimated using the time- or frequency-domain approaches is an average value of damping observed between some time intervals or a damping value observed at a particular frequency. This is in contrast to the damping present in vehicles, which is nonlinear. The dampers, in addition, traditionally have higher rebound damping than bump damping. Apart from this in-built nonlinearity, the construction and working of the damper may also result in further nonlinearity at larger velocities. The effective damping, therefore, may depend on the displacement and the velocity in a complex way. The damping of this nature can be estimated using the hysteresis curve. The forces transmitted through dampers

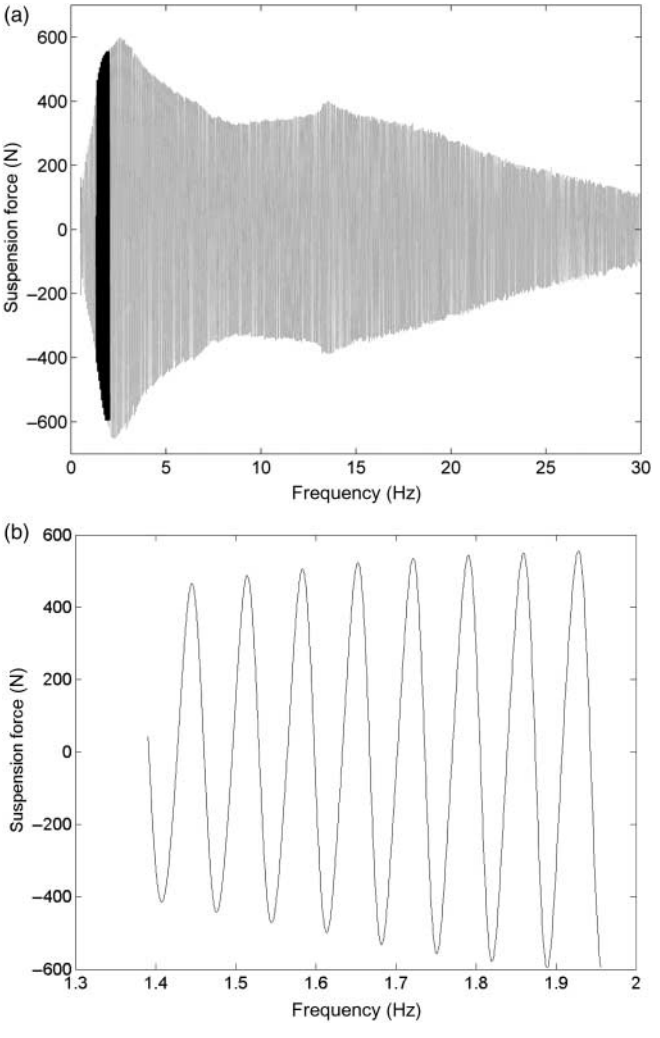


Figure 14. Variation in forces transmitted through front suspension as a function of frequency during frequency sweep (a) complete frequency range and (b) partial frequency range (1.4–1.9 Hz, shaded) used in estimating damper characteristics.

required for plotting the hysteresis curve can be estimated as all other parameters of the system are known (based on Section 4.2). Therefore, by knowing the suspension displacement and suspension stiffness, a hysteresis curve can be plotted for a particular cycle and from that bump and rebound damping can be calculated.

Figure 14a shows the front suspension force variation as a function of sweep frequency. Only a small part of these data are used in further analysis (shown shaded in Figure 14a), which is separately plotted in Figure 14b. The frequency range selected here is such that: (a) a mode is dominant allowing a single-DOF system assumption in the damping parameter estimation (the phase information, the dominance of damping related force and its velocity dependence are similar to that in a single-DOF systems) and (b) the damper goes through a large travel and significant velocity range; for example, the motion observed at the body bounce mode resonance frequency.

The plot of variation in force as a function of velocity provides information about the damping. For the front suspension, such a plot is shown in Figure 15. The variation does not follow the same path because there is a contribution from the springs to the suspension force. In addition, the curve is not an ellipse. This shows the presence of nonlinearity. There could be two sources of nonlinearity: (a) stiffness nonlinearity and (b) damping nonlinearity. Although the stiffness from the suspension springs is linear for the most part, some nonlinearity in the suspension stiffness could arise from linkages. In this study, in estimating the damping value, the stiffness is assumed to be linear; this may result in some errors in the estimated damping. The validity of the approach can be checked by the visual inspection of the damping curves; the method is expected to result in at least a good first estimate of the damping coefficients.

A consequence of the stiffness linearity assumption and associated discussion is that the nonlinearity must come from the damping element. The contribution from spring can be removed from the suspension force, and consequently, the plot of force variation as a function of velocity can be plotted. The variation of which is shown in Figure 16. For purely viscous damping, the path for increasing and decreasing the velocity would be the same; there appears to be a small contribution to the damping that does not follow viscous damping laws. The deviation seen may be attributed to frictional or joint effects. Apart from that, significantly, the back bone of the damper curve can be easily identified in the figure. Two dotted lines show the bump and rebound damping regions. As usually the case, for the vehicle used, the rebound

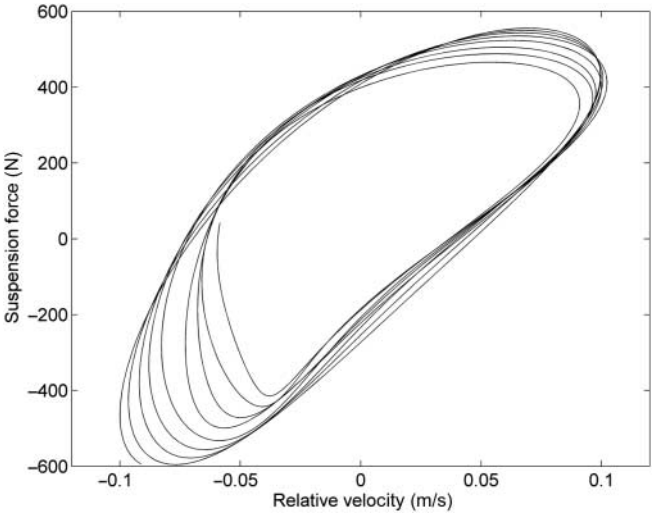


Figure 15. Variation in suspension force as a function of relative velocity for frequencies between 1.4 and 1.9 Hz.

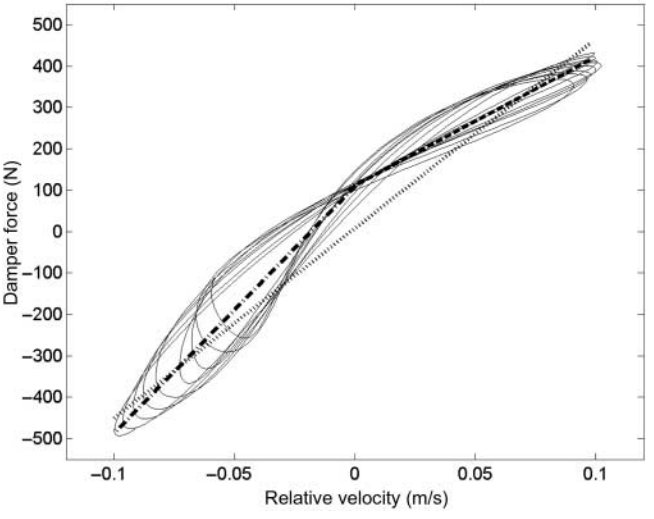


Figure 16. Damper curve showing damper force as a function of relative velocity. – –, bump (∼3000 Ns/m) and – · –, rebound (∼6000 Ns/m) part of damping curve; ....., average damping coefficient (∼4500 Ns/m).

damping coefficient is about twice as large as the bump damping coefficient. An approximate average linear damping line is also shown in Figure 16. It is worth noting that the average equivalent viscous damping value at a frequency can be found by taking the area within a curve completing one cycle where the force is plotted against the suspension displacement.

## 5. Discussion

Finally, the frequency average parameters calculated using: (a) above plots and (b) the discussion on the stiffnesses are listed in Table 2. For comparison, the physical parameters of the car that can be measured easily are listed in Table 3. The comparison of masses shows a good agreement; the overall mass of the car is estimated accurately to 1.2% of the actual value. Using the estimated parameters in four-DOF model, the bounce and pitch mode can be calculated. These natural frequencies are found to be 1.9 and 2.15 Hz, respectively. Although it is difficult to estimate the damping ratio, some measures of it can be obtained by the use of natural frequencies above. Using the estimated body mass, the body bounce natural frequency and the average damping coefficient (front and rear), an approximate of the damping ratio associated with body bounce mode can be estimated. In this case, it turns out to be 0.52. This ratio appears to be on the higher side; in any case, the vehicle tested is known for good handling but slightly poorer ride quality.

Table 2. Estimated suspension parameters of the car model.

| Parameter | Value |
|---|---|
| Body or sprung mass | 995 kg |
| Pitch inertia | 1170 kg m$^2$ |
| Front unsprung mass | 33 kg |
| Rear unsprung mass | 36 kg |
| Front suspension stiffness | 48,000 N/m |
| Rear suspension stiffness | 32,200 N/m |
| Average front damping | 4500 Ns/m |
| Average rear damping | 1660 Ns/m |

Table 3. Physical parameters of the car.

| Parameter | Value |
|---|---|
| Total mass of the car | 1147 kg |
| Static front wheel reaction | 3581.9 N |
| Static rear wheel reaction | 2023.7 N |
| Length from centre of gravity to the front wheel | 0.9 m |
| Length from centre of gravity to the rear wheel | 1.53 m |

## 6. Conclusions

A frequency-domain method was developed to estimate the suspension parameters used in the vehicle dynamic analysis. The formulation was arranged in the form of matrices of responses, parameters and forcing elements. The response matrix information was augmented by the introduction of dynamic and static constraint equations. The response and forcing elements were obtained by a test on a car excited using 4-post rig shakers. The time-domain approach was also developed; the implementation of such an approach on measured data revealed high sensitivity of the method to the measurement noise.

In the frequency-domain approach to reduce the measurement noise, the response and the forcing matrices were reformulated such that the elements were now frequency response functions. The drawback of the frequency-domain approach was its inability to identify nonlinear damping effectively. To over come this, a combination of frequency and the time-domain approach was proposed. The results of parameters found were less erroneous and also parameter estimates were smooth functions of frequency. The variations in parameters for different frequencies were explained using information of elements of the response matrix, which are dependent in this case on the modal resonant behaviour. The implementation of frequency responses as elements of the response matrix rather than responses, therefore, shows good potential in reducing the errors in estimations and error amplification during the matrix inversion. Finally, the damping curve was estimated, which for practical purposes provides the realistic bump and rebound damping.

## References

[1] T.D. Gillespie, *Fundamentals of Vehicle Dynamics*, Society of Automotive Engineers, USA, 1992.
[2] W.F. Milliken and D.L. Milliken, *Race Car Vehicle Dynamics*, Society of Automotive Engineers, USA, 1995.
[3] Y. Lin and W. Kortum, *Identification of system physical parameters for vehicle systems with nonlinear components*, Veh. Syst. Dyn. 20 (1991), pp. 354–365.
[4] K. Yi and K. Hedrick, *Observer based identification of nonlinear vehicle suspension parameters*, Proceedings of the American Control Conference, San Francisco, USA, 1993, pp. 711–715.
[5] R. Majjad, *Estimation of suspension parameters*, Proceedings of 1997 IEEE International Conference on Control Applications, Hartford, USA, 1997, pp. 522–527.
[6] P. Gaspar, Z. Szabo, and J. Bokor, *Parameter identification of a suspension system and road disturbance estimation*, Int. J. Veh. Syst. 2 (2007), pp. 128–137.
[7] J.K. Hammond, *Chapter 6: Fundamentals of signal processing*, in *Fundamentals of Noise and Vibration*, F. Fahy and J. Walker, eds., E & FN Spon, London, 1998.
[8] G.H. Golub and C.F. Van Loan, *Matrix Computations*, Johns Hopkins Studies in Mathematical Sciences, Baltimore, 1996.
[9] C. Hansen, *Rank-Deficient and Discrete Ill-Posed Problems: Numerical Aspects of Linear Inversion*, SIAM, Philadelphia, 1998.
[10] A.N. Thite and D.J. Thompson, *The quantification of structure-borne transmission paths by inverse methods. Part* 2 : *Use of regularization techniques*, J. Sound Vib. 264 (2003), 433–451.